analytical chemistry

Letter

pubs.acs.org/ac

# Rapid Quantification of Trimethylamine

Zheng Li, Hao Li,† Maria K. LaGasse, and Kenneth S. Suslick*

Department of Chemistry, University of Illinois at Urbana−Champaign, 600 S. Mathews Avenue, Urbana, Illinois 61801, United States

Supporting Information

**ABSTRACT:** Sensitive detection of trimethylamine both in aqueous and gaseous phases has been accomplished using an inexpensive colorimetric sensor array. Distinctive color change patterns provide facile discrimination over a wide range of concentrations for trimethylamine with >99% accuracy of classification. Calculated limits of detection are well below the diagnostically significant concentration for trimethylaminuria (fish malodor syndrome). The sensor array shows good reversibility after multiple uses and is able to cleanly discriminate trimethylamine from similar amine odorants. Portable sensing of trimethylamine vapors at ppb concentrations is described using a cell phone camera or a hand-held optoelectronic nose. Application of the sensor array in detecting mouth and skin odor as a potential tool for portable diagnosis of trimethylaminuria is also illustrated.

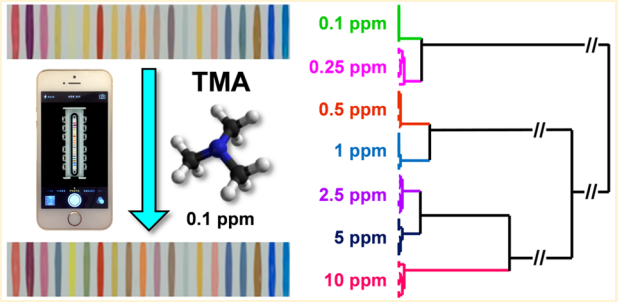


Trimethylaminuria (TMAU), also known as fish malodor syndrome, is a metabolic disorder characterized by excessive accumulation of malodorous trimethylamine (TMA) in breath, sweat, and urine;[1−4] TMAU is due to diminished activity of the flavin-containing monooxygenase-3 (FMO3) enzyme, which normally metabolizes TMA to the odorless trimethylamine *N*-oxide (TMAO). The prevalence of deficiency in FMO3 activity varies significantly among ethnic populations, ranging from <1% in the U.K. to 11% in New Guinea.[1,4] As such, there is a pressing need for a highly sensitive and selective sensor for the medical diagnosis of trimethylaminuria[1] and regular monitoring of TMA concentrations during treatment.

A number of analytical methods have been applied to detect TMA or other biogenic amines, including gas/high performance liquid chromatography,[5,6] ion mobility spectrometry,[7,8] quartz crystal microbalance,[9,10] and chemiresistive sensors (e.g., electronic nose techniques).[11−16] Most of these methods, however, require expensive instrumentation, complicated preparation of the sensors, lack of portability, or long times for analysis.

Traditional electronic nose technology suffers from sensor drift, poor selectivity, and environmental sensitivity (e.g., to changes in humidity or to interferents).[16−18] The interactions between analytes and sensors are generally dominated by physical sorption or a single chemical interaction, which gives a limited dimensionality to the resulting data. For example, gas sensors based on the weak interaction between TMA and Co(II)-imidazolate framework or $\alpha$-$Fe_2O_3$/$TiO_2$ nanostructure can only reach detection limits of several ppm.[19,20] Swager and co-workers have reported chemiresistive detectors made from Co porphyrin/carbon nanotube composites that exhibit sub-ppm sensitivity toward biogenic amines in 30 s; these sensors, however, cannot distinguish types of amines.[21] A multidimensional sensor array based on various chemical properties therefore becomes essential to distinguish among various potential biomarkers for analytical purposes.

In comparison, colorimetric sensor arrays have a broad analyte response, good environmental tolerance, and high selectivity; they are also small, fast, disposable, and can be analyzed using inexpensive equipment.[22−25] We have developed and improved an optoelectronic nose that uses colorimetric sensor arrays to detect and identify various analytes, ranging from toxic gases[26−29] to beverages,[30] microorganisms,[31] and even energetic materials.[32−35] Application of colorimetric arrays to the detection of amines for meat spoilage has also been recently reported.[36] Colorimetric sensor arrays rely on strong intermolecular interactions between the analytes and a chemically diverse set of cross-responsive dyes; the arrays use porous organically modified siloxanes (ormosils) or polymeric plasticizers[37−39] to immobilize the chemically responsive colorants, whose UV−vis absorbances are altered by Brønsted and Lewis acid−base interactions, redox reactions, vapochromism/solvatochromism, and so forth.

Herein, we report an inexpensive and sensitive colorimetric method for rapid detection of gaseous and aqueous TMA. All 20 sensor elements were rigorously optimized in their formulations by adjusting the dye amount and pH to enhance their sensitivity, and three main classes of colorants were incorporated (Table S1): (1) metal-containing dyes (e.g., Zn(II) metalloporphyrin) that respond to Lewis basicity to simulate mammalian olfactory receptors,[40,41] (2) pH indicators that respond to Brønsted basicity, and (3) dyes with large

**Received:** March 24, 2016
**Accepted:** May 13, 2016
**Published:** May 24, 2016

  

DOI: 10.1021/acs.analchem.6b01170
*Anal. Chem.* 2016, 88, 5615−5620

permanent dipoles (i.e., vapochromic dyes) that respond to local polarity.[42,43] We make use of highly porous sol−gel formulations to obtain a better responsiveness to gaseous analytes as well as the ideal hydrophobicity of the matrix to minimize the dissolution of the dyes during liquid sensing.

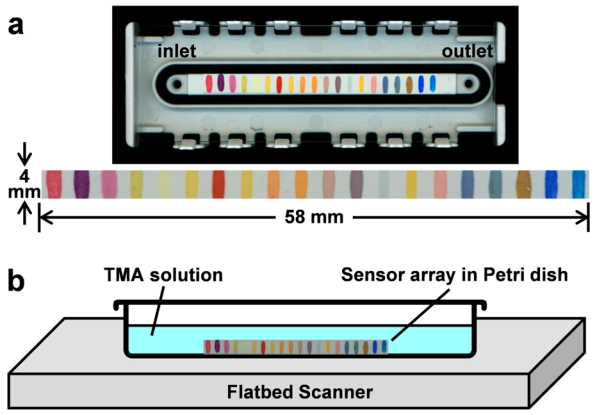


**Figure 1.** Colorimetric sensor array for TMA detection. (a) Linearized 20-element sensor array for vapor detection; the array was mounted on a polycarbonate cartridge with an O-ring placed in a groove and a glass slide cover in place, which provides an ideal flow path for analytes and a flow volume of <180 $\mu$L (77 × 4.5 × 0.5 mm). (b) Schematic of the experimental setup consisting of a closed Petri dish containing 10 mL of a buffered aqueous TMA solution, an array positioned in the solution, and an ordinary flatbed scanner for imaging.

The arrays were linearized for improved gas flow path and printed robotically (Figure S1), then mounted on a snap-together, disposable cartridge (Figure 1a); the low dead volume of this configuration greatly improves the array response time. Digital images of the arrays were acquired before and after exposure to dilute gas mixtures or aqueous solutions using an ordinary flatbed scanner (Epson Perfection V600, Figure 1b and Figure S2). Color difference maps were generated from changes in red, green, and blue values of each spot upon exposure to analytes. Figure 2 shows sensor array responses to a series of concentrations of gaseous and aqueous TMA after 2 min exposure: significant color changes were observed by the naked eye even at sub-ppm levels (Figure S3). The biggest responses are from solvatochromic dyes (spots 1 and 2), pH indicators (spots 4−6 and 8−11), and metal-containing dyes (spots 16−18), which reflects the changes in local polarity, Brønsted basicity, and Lewis basicity, respectively, induced by the presence of TMA. Color difference maps as a function of TMA concentration are readily distinguished from one another even by eye before any statistical analysis. The response curves for both gaseous and aqueous TMA detection are more than 90% equilibrated within 2 min at most concentrations based on total array response in Euclidean distance (Figure S4). Although the array is meant to be a disposable, it shows excellent reversibility between different concentrations of TMA (Figure S5).

For a semiquantitative analysis of the sensor array responses, we made use of a standard chemometric approach, hierarchical cluster analysis (HCA),[44,45] to group color changes by concentration. The advantages of HCA are that it deals well with high dimensional data and is inherently model-free in its analysis (i.e., unsupervised). The clustering of vectors is based on their positions in the 60-dimensional Euclidean space (i.e., the changes in RGB values for each of the 20 sensor spots). Figure 3 shows the HCA dendrogram for 2 min exposure to both gaseous and aqueous TMA. In septuplicate trials, all 15 TMA concentrations and two controls show tight clustering without error in clustering 119 cases. Even in the low concentration cases (5 and 10 $\mu$M of aqueous TMA; 0.1 and 0.25 ppm of gaseous TMA), good separation of clusters was still observed with no misidentifications.

A more sophisticated, but supervised, classification method, support vector machine (SVM) analysis, was used to create optimized classifiers. Unlike clustering methods such as HCA, SVM is a predictive method designed to classify new incoming

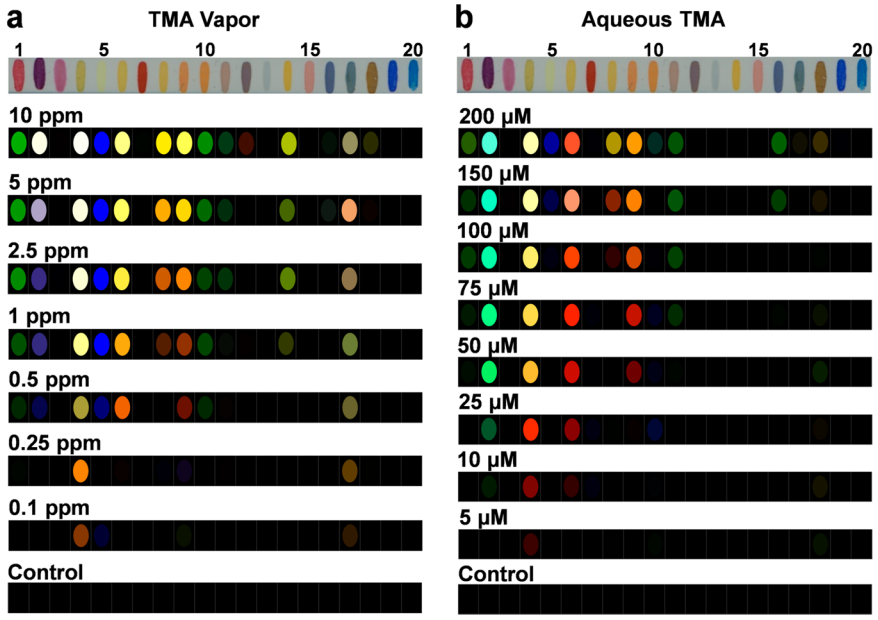


**Figure 2.** Average responses of the sensor array to different concentrations of (a) gaseous and (b) aqueous TMA and controls, each run in septuplicate trials. For visualization, the color range is expanded from 4 to 8 bits per color (i.e., RGB color range of 4−19 expanded to 0−255).



DOI: 10.1021/acs.analchem.6b01170
*Anal. Chem.* 2016, 88, 5615−5620

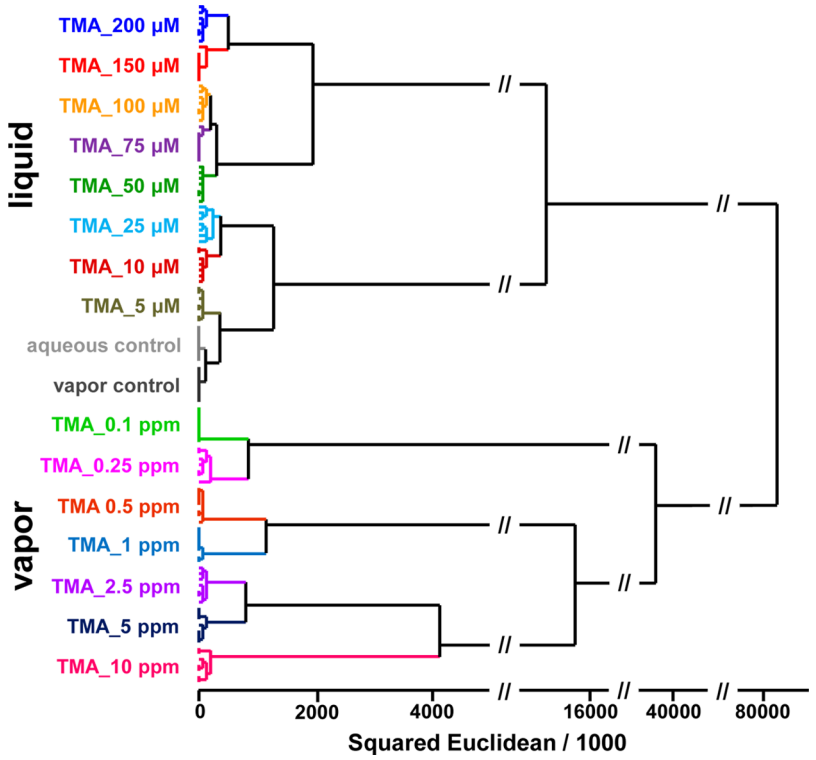


**Figure 3.** Dendrogram of hierarchical cluster analysis for TMA at different concentrations in gases or in solutions with two controls; 119 trials. All of the concentrations were clearly discriminable from each other.

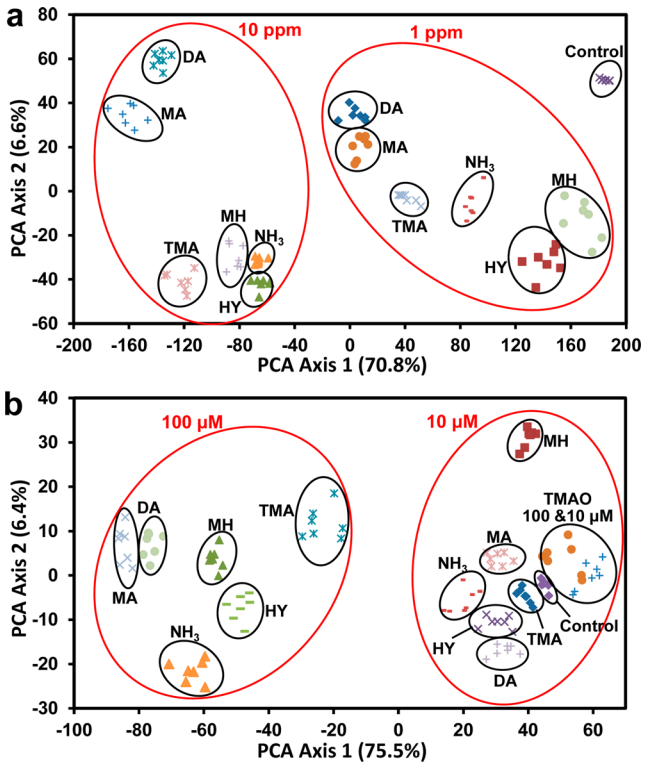


**Figure 4.** Two-dimensional principal component analysis score plot for septuplicate trials of (a) gaseous amines at 1 and 10 ppm and a control and (b) aqueous amines at 10 and 100 $\mu$M and a control. Overlap is observed only between 10 and 100 $\mu$M TMAO.

data that is not part of the training database. SVM classification is based on pairwise class prediction and focuses on the data most likely to be misclassified (i.e., the so-called support vectors) using a specific transformation function (kernel) that best separates the data for any given pair of classes. Classification accuracy can be estimated using cross-validation methods that split the database and create classifiers based on training and evaluation data subsets. SVM results using a leave-one-out permutation method of cross-validation are shown in Table S2. No misclassifications were found among either gaseous or aqueous samples, i.e., the error rate of predictive classification is <1% out of 119 trials.

We estimate the limits of detection (LODs) for gaseous and aqueous TMA by extrapolating from the observed array responses at relevant concentrations. We define the LOD as the concentration needed to give three times the S/N versus background for the largest response among the 60 color difference vectors. The calculated LODs for TMA are 4 ppb in gas phase and 2.3 $\mu$M in the aqueous media (Figure S6). The LOD of TMA gas is comparable to the threshold of human olfactory receptors (2.5 ppb),[46] whereas that of aqueous TMA is well below the threshold for the appearance of fish malodor symptoms (10 $\mu$g/mL, i.e., 169 $\mu$M).[47] Our LODs are also well below the NIOSH/OSHA permissible exposure limit (PEL) of TMA, i.e., 10 ppm for long-term exposure; as a toxic gaseous irritant, TMA can cause health issues such as headaches, nausea, and skin burns.

For the two LODs obtained in different phases to be compared, Henry's law was employed to calculate the gaseous equivalent of the aqueous concentration. Using the appropriate Henry solubility constant (i.e., 0.47 mol $m^{-3}$ $Pa^{-1}$),[48,49] the equilibrium partial pressure of TMA vapor above the aqueous solution at its LOD is estimated to be ~50 ppb, which is ~10 times higher than the gaseous LOD. This reflects the effect of interference from water on the response of the sensor array.



DOI: 10.1021/acs.analchem.6b01170
*Anal. Chem.* 2016, 88, 5615−5620

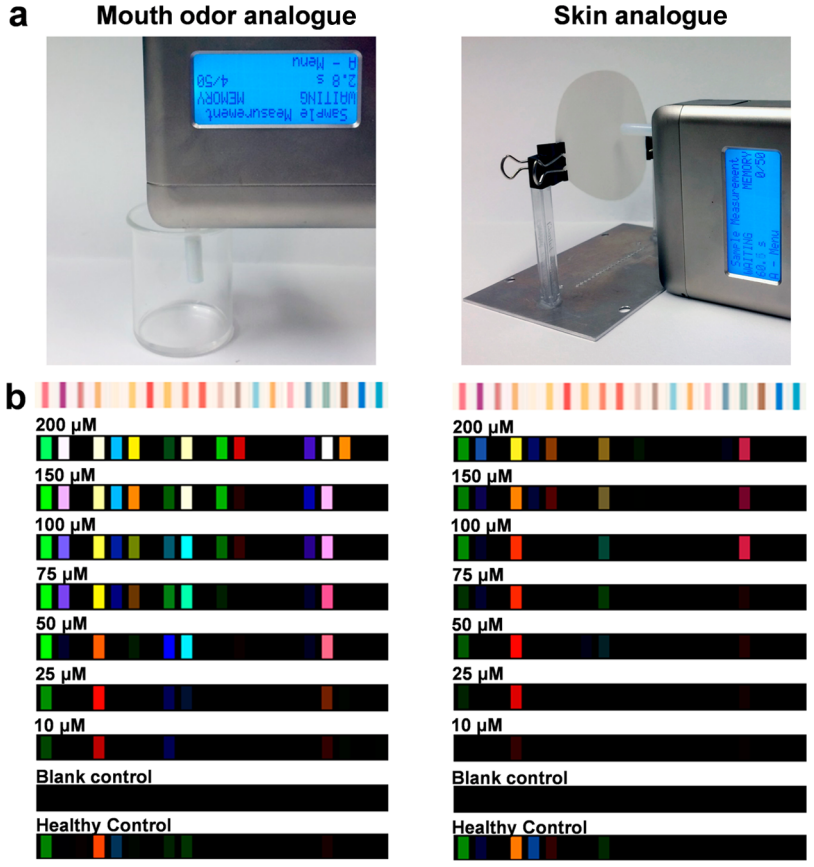


**Figure 5.** (a) Experimental setup for mouth or skin odor simulation using the hand-held device; headspace gas was sampled from 2 mL TMA solution in a beaker for the mouth odor test or from filter paper soaked in 0.5 mL of TMA solution for the skin odor test. (b) Averaged sensor array response to different concentrations of TMA and controls; healthy controls were collected from the author (from mouth and axilla for (a) and (b), respectively). Each sample was collected in septuplicate. For display purposes, S/N ratios of 3−10 were scaled on an 8-bit RGB color scale (i.e., 0−255).

Although LODs are well-defined mathematically, they represent only the point at which the array detects something, but does not tell the identity of the analyte. The point at which one can discriminate one analyte from another is the limit of recognition (LOR), which is inherently less well-defined because it depends upon the library of analytes among which one wishes to differentiate. Here, we have examined five representative amines (ammonia, dimethylamine (DA), methylamine (MA), hydrazine (HY), and methylhydrazine (MH)) as low molecular weight analogues to TMA as well as its *N*-oxide metabolite, TMAO; all analytes were tested both in aqueous media and as gases (except the solid TMAO) at two concentrations (10 and 100 $\mu$M for solutions; 1 and 10 ppm for gases). The HCA dendrogram shows that all gaseous amines are perfectly clustered (Figue S7); among the aqueous samples, the array data does not differentiate between the 10 and 100 $\mu$M trials of TMAO (Figure S7), presumably due to the relatively low sensitivity of our sensor to TMAO, which is only a weak base[50] ($pK_a$ = 4.7). It is clear that the sensor array is able to distinguish TMA from other amines or TMAO in both gaseous and aqueous phases, and we conclude that the LOR for TMA relative to five similar amino odorants is well below 1 ppm in the gas phase and 10 $\mu$M in aqueous media.

For the array's specificity toward TMA to be better elucidated, principal component analysis (PCA)[51,52] was performed to give a measurement of the dimensionality of the database. A relatively high dimensionality among various amines at two concentrations was expected and indeed observed (Figure S8): 10 dimensions are required to capture 90% of the total variance of all gaseous samples and 8 dimensions for aqueous ones, which is consistent with the wide range of analyte chemical properties probed by the sensor array. Despite the high dimensionality, good discrimination is provided even by just the first two principal components, as shown in Figure 4. As with the HCA, all gaseous analytes were differentiable from each other, and all aqueous analytes were differentiable except for 10 and 100 $\mu$M TMAO.

For point of care diagnosis, portability of the imaging device is paramount. To that end, we have very recently developed a hand-held reader[53] that uses a diaphragm micropump to sample analyte gases and a color contact image sensor (CIS) to collect colorimetric data; the hand-held reader has shown promising applications in the discrimination of homemade explosives.[33,35] In addition, we have also examined the use of a cell phone camera, which has the added advantage of ready availability; cell phone imaging has just begun to find analytical applications.[54,55] We therefore collected sensor array responses at designated concentrations of TMA vapors using our hand-held reader and an iPhone 5s (Figure S9), which both show similar sensor response patterns to those collected by the flatbed scanner (Figure S10); HCA gives 100% accuracy of clustering by scanning methods and then by TMA concentration in 147 trials (Figure S11). LOD measurements show the sensitivity of


DOI: 10.1021/acs.analchem.6b01170
*Anal. Chem.* 2016, 88, 5615−5620

three devices to TMA vapors: hand-held scanner, 3 ppb; flatbed, 4 ppb; cellphone, 6 ppb (Figure S12).

In a simulation of skin or mouth odor test for diagnosis of trimethylaminuria, we used this hand-held reader to monitor the volatiles from filter papers soaked in TMA solutions or headspace TMA vapors (Figure 5). Mouth odor simulations generally gain higher responses than skin ones after two min of exposure. In patients with trimethylaminuria, the threshold for fish malodor symptoms is defined at TMA concentrations in urine of 10 $\mu$g/mL, i.e., 169 $\mu$M.[47] Our simulations (Figure 5 and Figure S13) show clear discrimination among diagnostically significant concentrations of TMA, blank, and healthy controls with calculated detection limits of ~5 $\mu$M for mouth odor simulations and ~2 $\mu$M for skin ones, which are comparable to the results obtained from the flatbed scanner.

In conclusion, we have developed a simple and portable colorimetric sensor for the detection of trimethylamine from vapor or aqueous solution using various imaging devices with relevance to point of care diagnosis of a genetic and metabolic disease, trimethylaminuria (TMAU). Apparent color differences shown by the sensor arrays allow for a quick identification of trimethylamine concentration even by eye. LODs for trimethylamine in the gas phase are a few ppb and in aqueous phase a few $\mu$M, which are well below the diagnostically significant concentration for TMAU. We have examined new methods for portable acquisition of colorimetric data and, importantly, made comparisons between them (e.g., flat bed scanner vs cell phone camera vs customized line scanner hand-held imagers). Principal component analysis, hierarchical cluster analysis, and support vector machine analysis all show excellent discriminatory power over a wide range of concentrations for three different imaging methods (including cell phone camera) with error rates <1%. The sensor is robust and reusable after multiple exposures. The optoelectronic nose promises to be a useful point of care device for rapid, quantitative diagnosis and monitoring of trimethylamine levels for patients with trimethylaminuria.

## ■ ASSOCIATED CONTENT

### Supporting Information

The Supporting Information is available free of charge on the ACS Publications website at DOI: 10.1021/acs.analchem.6b01170.

Tables of dye formulations, experimental details, sensor response graphs, statistical analysis, and all raw data (PDF)

## ■ AUTHOR INFORMATION


### Corresponding Author

*E-mail: ksuslick@illinois.edu.

### Present Address

†H.L.: University of Science and Technology of China, Hefei, Anhui 230026, P. R. China


### Notes

The authors declare no competing financial interest.

## ■ ACKNOWLEDGMENTS

The authors acknowledge the U.S. National Science Foundation (CHE-1152232) for financial support and a generous gift from the Procter and Gamble Foundation. We also thank Drs. Xiaole Mao and Sherman Faiz for helpful discussions.

## ■ REFERENCES


(1) Mackay, R. J.; McEntyre, C. J.; Henderson, C.; Lever, M.; George, P. M. *Clin. Biochem. Rev.* **2011**, *32*, 33−43.
(2) Ferreira, F.; Esteves, S.; Almeida, L. S.; Gaspar, A.; da Costa, C. D.; Janeiro, P.; Bandeira, A.; Martins, E.; Teles, E. L.; Garcia, P.; Azevedo, L.; Vilarinho, L. *Gene* **2013**, *527*, 366−370.
(3) Miller, N. B.; Beigelman, A.; Utterson, E.; Shinawi, M. *JIMD Reports* **2013**, *12*, 11−15.
(4) Mitchell, S. C.; Zhang, A. Q.; Barrett, T.; Ayesh, R.; Smith, R. L. *Pharmacogenetics* **1997**, *7*, 45−50.
(5) Zaitsu, K.; Katagi, M.; Kamata, H.; Kamata, T.; Shima, N.; Miki, A.; Iwamura, T.; Tsuchihashi, H. *J. Mass Spectrom.* **2008**, *43*, 528−534.
(6) Cháfer-Pericás, C.; Campíns-Falcó, P.; Herráez-Hernández, R. *Talanta* **2006**, *69*, 716−723.
(7) Wang, Q.; Xie, Y.-F.; Zhao, W.-J.; Li, P.; Qian, H.; Wang, X.-Z. *Anal. Methods* **2014**, *6*, 2965−2972.
(8) Bota, G. M.; Harrington, P. B. *Talanta* **2006**, *68*, 629−635.
(9) Li, G.; Zheng, J.; Ma, X.; Sun, Y.; Fu, J.; Wu, G. *Sensors* **2007**, *7*, 2378.
(10) Wang, X.; Ding, B.; Yu, J.; Si, Y.; Yang, S.; Sun, G. *Nanoscale* **2011**, *3*, 911−915.
(11) Lee, S. H.; Lim, J. H.; Park, J.; Hong, S.; Park, T. H. *Biosens. Bioelectron.* **2015**, *71*, 179−185.
(12) Yang, R.; Huang, X.; Wang, Z.; Zhou, Y.; Liu, L. *Sens. Actuators, B* **2010**, *145*, 474−479.
(13) Woo, H.-S.; Na, C. W.; Kim, I.-D.; Lee, J.-H. *Nanotechnology* **2012**, *23*, 245501.
(14) Kwak, C.-H.; Woo, H.-S.; Lee, J.-H. *Sens. Actuators, B* **2014**, *204*, 231−238.
(15) Zhang, R.; Wang, L.; Deng, J.; Zhou, T.; Lou, Z.; Zhang, T. *Sens. Actuators, B* **2015**, *220*, 1224−1231.
(16) Stitzel, S. E.; Aernecke, M. J.; Walt, D. R. *Annu. Rev. Biomed. Eng.* **2011**, *13*, 1−25.
(17) Röck, F.; Barsan, N.; Weimar, U. *Chem. Rev.* **2008**, *108*, 705−725.
(18) Nakamoto, T.; Ishida, H. *Chem. Rev.* **2008**, *108*, 680−704.
(19) Chen, E.-X.; Fu, H.-R.; Lin, R.; Tan, Y.-X.; Zhang, J. *ACS Appl. Mater. Interfaces* **2014**, *6*, 22871−22875.
(20) Lou, Z.; Li, F.; Deng, J.; Wang, L.; Zhang, T. *ACS Appl. Mater. Interfaces* **2013**, *5*, 12310−12316.
(21) Liu, S. F.; Petty, A. R.; Sazama, G. T.; Swager, T. M. *Angew. Chem., Int. Ed.* **2015**, *54*, 6554−6557.
(22) Rakow, N. A.; Suslick, K. S. *Nature* **2000**, *406*, 710−714.
(23) Askim, J. R.; Mahmoudi, M.; Suslick, K. S. *Chem. Soc. Rev.* **2013**, *42*, 8649−8682.
(24) Diehl, K. L.; Anslyn, E. V. *Chem. Soc. Rev.* **2013**, *42*, 8596−8611.
(25) McDonagh, C.; Burke, C. S.; MacCraith, B. D. *Chem. Rev.* **2008**, *108*, 400−422.
(26) Rakow, N. A.; Sen, A.; Janzen, M. C.; Ponder, J. B.; Suslick, K. S. *Angew. Chem., Int. Ed.* **2005**, *44*, 4528−4532.
(27) Lim, S. H.; Feng, L.; Kemling, J. W.; Musto, C. J.; Suslick, K. S. *Nat. Chem.* **2009**, *1*, 562−567.
(28) Feng, L.; Musto, C. J.; Kemling, J. W.; Lim, S. H.; Suslick, K. S. *Chem. Commun.* **2010**, *46*, 2037−2039.
(29) Janzen, M. C.; Ponder, J. B.; Bailey, D. P.; Ingison, C. K.; Suslick, K. S. *Anal. Chem.* **2006**, *78*, 3591−3600.
(30) Zhang, C.; Bailey, D. P.; Suslick, K. S. *J. Agric. Food Chem.* **2006**, *54*, 4925−4931.
(31) Carey, J. R.; Suslick, K. S.; Hulkower, K. I.; Imlay, J. A.; Imlay, K. R. C.; Ingison, C. K.; Ponder, J. B.; Sen, A.; Wittrig, A. E. *J. Am. Chem. Soc.* **2011**, *133*, 7571−7576.
(32) Li, Z.; Jang, M.; Askim, J. R.; Suslick, K. S. *Analyst* **2015**, *140*, 5929−5935.
(33) Askim, J. R.; Li, Z.; LaGasse, M. K.; Rankin, J. M.; Suslick, K. S. *Chemical Science* **2016**, *7*, 199−206.
(34) Berliner, A.; Lee, M.-G.; Zhang, Y.; Park, S. H.; Martino, R.; Rhodes, P. A.; Yi, G.-R.; Lim, S. H. *RSC Adv.* **2014**, *4*, 10672−10675.
(35) Li, Z.; Bassett, W. P.; Askim, J. R.; Suslick, K. S. *Chem. Commun.* **2015**, *51*, 15312−15315.




DOI: 10.1021/acs.analchem.6b01170
*Anal. Chem.* 2016, 88, 5615−5620

(36) Xiao-wei, H.; Zhi-hua, L.; Xiao-bo, Z.; Ji-yong, S.; Han-ping, M.; Jie-wen, Z.; Li-min, J.; Holmes, M. *Food Chem.* **2016**, *197*, 930−936.
(37) Kemling, J. W.; Suslick, K. S. *Nanoscale* **2011**, *3*, 1971−1973.
(38) Feng, L.; Musto, C. J.; Suslick, K. S. *J. Am. Chem. Soc.* **2010**, *132*, 4046−4047.
(39) LaGasse, M. K.; Rankin, J. M.; Askim, J. R.; Suslick, K. S. *Sens. Actuators, B* **2014**, *197*, 116−122.
(40) Wang, J.; Luthey-Schulten, Z. A.; Suslick, K. S. *Proc. Natl. Acad. Sci. U. S. A.* **2003**, *100*, 3035−3039.
(41) Suslick, K. S. *MRS Bull.* **2004**, *29*, 720−725.
(42) Rankin, J. M.; Zhang, Q.; LaGasse, M. K.; Zhang, Y.; Askim, J. R.; Suslick, K. S. *Analyst* **2015**, *140*, 2613−2617.
(43) Feng, L.; Musto, C. J.; Kemling, J. W.; Lim, S. H.; Zhong, W.; Suslick, K. S. *Anal. Chem.* **2010**, *82*, 9433−9440.
(44) Hair, J. F.; Black, B.; Babin, B.; Anderson, R. E.; Tatham, R. L. *Multivariate Data Analysis*, 6th ed.; Prentice Hall: New York, 2005.
(45) Janata, J. *Principles of Chemical Sensors*, 2nd ed.; Springer: New York, 2009.
(46) Devos, M.; Patte, F.; Rouault, J.; Laffort, P.; Van Gemert, L. J. *Standardized Human Olfactory Thresholds*; Oxford University Press: New York, 1990.
(47) Mitchell, S. C.; Smith, R. L. *Drug Metab. Dispos.* **2001**, *29*, 517−521.
(48) Sander, R. *Atmos. Chem. Phys.* **2015**, *15*, 4399−4981.
(49) Nirmalakhandan, N.; Brennan, R. A.; Speece, R. E. *Water Res.* **1997**, *31*, 1471−1481.
(50) Singh, R.; Haque, I.; Ahmad, F. *J. Biol. Chem.* **2005**, *280*, 11035−11042.
(51) Johnson, R. A.; Wichern, D. W. *Applied Multivariate Statistical Analysis*, 6th ed.; Prentice Hall: New York, 2007.
(52) Jolliffe, I. T. *Principal Component Analysis*; Springer: New York, 2002.
(53) Askim, J. R.; Suslick, K. S. *Anal. Chem.* **2015**, *87*, 7810−7816.
(54) Liu, X. Y.; Lin, T. Y.; Lillehoj, P. B. *Ann. Biomed. Eng.* **2014**, *42*, 2205−2217.
(55) Jia, M.-Y.; Wu, Q.-S.; Li, H.; Zhang, Y.; Guan, Y.-F.; Feng, L. *Biosens. Bioelectron.* **2015**, *74*, 1029−1037.



DOI: 10.1021/acs.analchem.6b01170
*Anal. Chem.* 2016, 88, 5615−5620